Computers and Electronics in Agriculture
29 (2000) 59–72

Computers and electronics in agriculture

www.elsevier.com/locate/compag

# Discrimination of soybean leaflet shape by neural networks with image input

Mari Oide *, Seishi Ninomiya

*Department of Information Science and Technology, National Agriculture Research Center, 3-1-1 Kannondai, Tsukuba, Ibaraki 305-8666, Japan*

Accepted 22 May 2000

**Abstract**

It is necessary to correctly evaluate intra- and inter-specific variations for the efficient collection and preservation of genetic resources, and leaf shape is one of the important characteristics to be evaluated. It has been thought that a more consistent and quantitative method should be introduced to aid in the processes of practical discrimination. Several researchers have suggested leaf shape evaluation methods using shape features, and these methods have shown good results. The shape features selected in these methods have differed from one method to another, and new shape features must be redefined when these methods are applied to new cases. The processes for defining and extracting shape features are ad hoc. We, therefore, have attempted to develop a generalized model that requires neither the definition nor extraction of any shape features; the method uses neural networks into which leaf shape images are input. In this study, we applied a Hopfield model and a simple perceptron to the varietal discrimination of individual leaflet shapes of 364 soybean leaflets of 38 varieties. In the examination of up to ten varieties, the discriminant error of the neural networks with image input was satisfactorily low even under cross validation. We, therefore, concluded that this model works quite well for quantitative varietal discrimination in the case of soybean leaflets. The advantage of requiring neither the definition nor extraction of any shape features makes us expect that this model will be widely applicable to other cases, and we will attempt to verify this applicability. © 2000 Elsevier Science B.V. All rights reserved.

*Keywords:* Image analysis; Leaf shape; Neural network; Shape discrimination; Soybean leaflet

* Corresponding author. Tel.: +81-298-38-8948; fax: +81-298-38-8551.
*E-mail address:* oidemari@narc.affrc.go.jp (M. Oide).


PII: S0168-1699(00)00136-8

## 1. Introduction

Exact shape evaluation of intra- and inter-specific variations is essential for the classification process in collecting and preserving genetic resources, although molecular-biological approaches are becoming popular. Classificatory criteria based on qualitative shape features has been established, and people have carried out the discrimination work in accordance with these criteria. There is some possibility, however, that such discrimination is incorrect and inconsistent. Quantitative shape evaluation is necessary to carry out correct and consistent shape discrimination. An easy and automatic method to quantitatively measure shape is also necessary to save labor. Leaf shape is one of the characteristics to be evaluated and that plays an important role in the classification process. Therefore, it is necessary to develop a method that can easily measure and quantitatively evaluate leaf shape, and several researchers have attempted to establish methods for the quantitative measurement and discrimination of leaf shape.

Carneiro and Lima (1987) have suggested that the distance between the landmarks of leaf shape could be indicative of the similarities in grapevine (*Vitis vinifera* L.) leaf shape among varieties and habitats. Dickinson et al. (1987) have shown that the truss network (connected landmarks of leaf shape) and the sheared principal components are useful in expressing variations in hawthorn (*Crataegus*) hybrids and American larch (*Larix laricina* Koch) leaf shape. McLellan (1990) has shown that leaf shape variations in *Begonia dregei* (Begoniaceae) at different stages of growth can be expressed by the distances between landmarks of leaf shape. Sawada (1992) has developed a leaf shape index (aspect ratio) and has shown that this index can describe variations in soybean (*Glycine max* L. Merr.) leaflet shape. Wu (1994) has indicated that a leaf shape index (aspect ratio) can reasonably represent variations in tobacco (*Nicotiana tabacum* L.) leaves at different stages of growth. Gerber and Les (1994) have shown that variations in the leaf shape of water milfoil (*Myriophyllum*) can be described by a regression of the surface area and volume. Yonekawa et al. (1996) have shown that 11 simple shape features (e.g. convex hull, diameter of an inscribed circle) can identify Makino's idealized 50 leaf shapes (Makino, 1961). Guyer et al. (1993) have succeeded in classifying leaf shape into 40 types, extracting 17 shape features (e.g. principal axis moment, complexity) from images taken in the natural field environment. Ingrouille and Laird (1986), Jensen (1990) have examined methods for discriminating oak (*Quercus*) species based on leaf shape features. The former surveyed and compared five statistical analyses of 27 leaf shape features (e.g. auricle size, lobe depth ratio), showing that the principal component analysis was superior to other analyses. The latter compared the fit analyses using the landmarks of oak leaves, showing that the rotational-fit analysis expressed the affine components better than the least-square and resistant-fit analysis. Ray (1992) has developed a landmark eigenshape analysis as an improvement of eigenshape analysis, which describes the leaf shape of *Syngonium podophyllum* Schott (Araceae) with landmarks to discriminate leaf shape.

The above cases show that shape features are extremely powerful in discriminating difference in leaf shape. Selected shape features, however, have differed from one method to another, and new shape features must be redefined when these methods are applied to other cases. The process of identifying these features is ad hoc, making it necessary to inefficiently repeat the same process again and again.

On the other hand, shape evaluation models that do not require shape features have also been developed. Fujita et al. (1992) have suggested a model for bull's-eye disease diagnosis using a neural network into which bull's-eye images were input. Oide and Ninomiya (1998) have suggested a neural network with image input to evaluate soybean plant shape for selection in breeding. In both cases, satisfactory discriminant error was obtained for their respective materials.

In this study, we suggest a leaf shape evaluation model requiring neither definition nor extraction of shape features; the model uses a neural network into which leaf shape images are input. We have examined the neural networks for varietal discrimination, using soybean leaflet shape as a case study.

Fujita et al. (1992) have examined the use of a multilayer perceptron (MLP, Rumelhart et al., 1986) in classifying bull's-eye images into eight classes. This classification problem was rather simple because the inter-class similarity was low. Therefore, they could find an optimal MLP structure for correct discrimination by examining the number of hidden unites of the one-hidden-layer MLP. Adopting MLPs, Oide and Ninomiya (1998) have searched an optimal MLP structure for correct evaluation of soybean plant shape, changing the number of layers, input units, hidden units and output units. Although this was a classification problem with only three classes, they were not able to find an optimal structure strictly.

In this study, the leaf shape was classified into more than three classes (the maximum number of classes was 38, the same as the number of soybean varieties), and it was assumed that it was difficult to determine the MLP structure for correct discrimination. We, therefore, adopted a Hopfield model (HM, Hopfield, 1982) and a simple perceptron (SP, Rosenblatt, 1962), expecting an easy determination of neural network structures.

## 2. Materials and methods

We used 364 individual soybean leaflet data of 38 varieties, whose contours had been described with standardized elliptic Fourier coefficients (Furuta et al., 1995; Hadipoentyanti et al., 1996). The standardization made the contours into translation, rotation and size invariant. The contour standardization was necessary for the neural networks to evaluate size-invariant shape itself. We obtained the coordinates of $T$ points on the leaflet contour, using the standardized elliptic Fourier coefficients. $T$ was sufficiently large to maintain the neighboring pixel connectedness. In this study, we set $T$ to be $4M$ when the size of the image on which the contour was drawn was $M \times M$. The reconstructed contour coordinates by the standardized elliptic Fourier coefficients became the real number between $-1$ and $+1$. Therefore, we carried out similar transformation of the contour coordinates so that the closed interval $[-1, +1]$ was transformed to $[0, M]$, and rounded them off to integers. The closed contour was thereupon drawn on the $M \times M$-pixel image.

An individual leaflet shape (ILS) image was obtained by painting the inside of the contours drawn with the standardized elliptic Fourier coefficients. The ILS images were used as test data to evaluate the discrimination error. We also obtained a mean leaflet shape (MLS) and a leaflet shape distribution (LSD) as supervisory data. The MLS was defined as the contour drawn with average standardized elliptic Fourier coefficients for an individual leaflet within a variety. The LSD was defined as the average image over ILSs within a variety. The ILS and MLS were binary images, and we set the pixels of the leaves and backgrounds as $+1$ and $-1$, respectively. The LSD was a gray level image, and we established a real number between $-1$ and $+1$ for each pixel. We examined three different sizes of images as input data for the neural networks, e.g. $16 \times 16$, $32 \times 32$ or $64 \times 64$ pixels. Fig. 1 shows the ILS, MLS, and LSD images of a variety.

We adopted two types of neural network models; one was a Hopfield model (HM, Hopfield, 1982), and the other was a simple perceptron (SP, Rosenblatt,

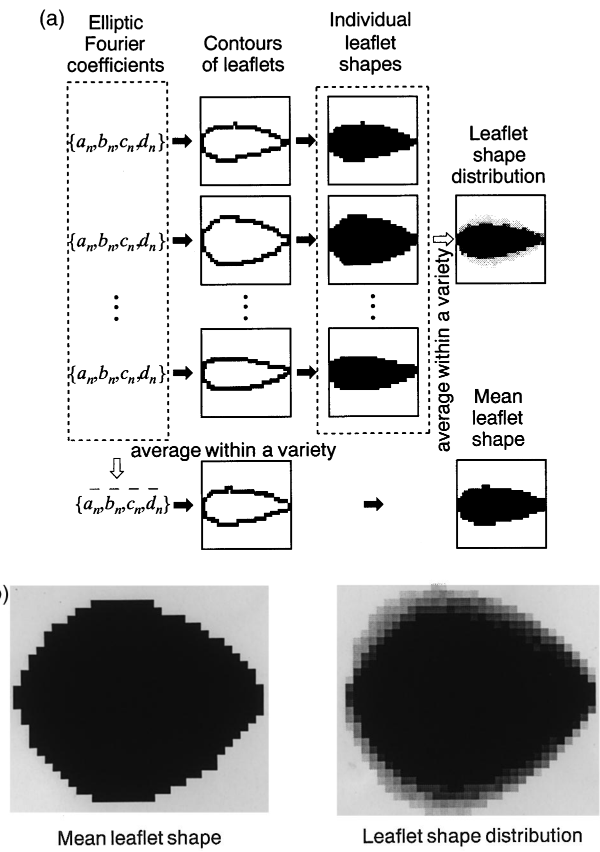


Fig. 1. Individual leaflet shapes, mean leaflet shape, and leaflet shape distribution: (a) individual leaflet shape, mean leaflet shape, and leaflet shape distribution image of a variety; (b) Example of mean leaflet shape and leaflet shape distribution of a variety.

1962). We programmed neural network simulator software using the C language of HP/CONVEX Exemplar SPP1600/XA-32 (Hewlett–Packard Inc., Palo Alto, CA). The software supported a large memory for storing images, fast processing by a minimum set of the essential neural network's functions, and unlimited setup of neural network parameters. No other software meeting these conditions was commercially available to us. We used neural networks with linear units, as they provided the simplest possible structure for the first step of the neural network examination in our problems.

The HM consisted of the same number of linear units as the number of pixels of the input image in this study. The dynamics of the HM were expressed as

$$u_i(t) = \xi_i^\lambda, \quad \text{for } i = 1,\cdots, N,\ \lambda = 1,\cdots, P, \quad t = 0 \tag{1}$$

$$u_i(t+1) = \sum_{j=1}^{N} w_{ij} u_j(t), \quad \text{for } i = 1,\cdots, N, \quad t = 0, 1,\cdots \tag{2}$$

where $N$ was the number of pixels, $P$ was the number of training varieties, $u_i(t)$ was the output of the $i$th unit at time $t$, $w_{ij}$ was the connection strength from the $j$th to the $i$th unit, and $\xi_i^\lambda$ was the $i$th pixel value of the $\lambda$th supervisory image. All units were updated synchronously with $t$. The target output was the same as the corresponding supervisory image, so that the HM worked as an associative memory. That is, the relationship between the supervisory images and their target outputs were

$$\xi_i^\lambda = \sum_{j=1}^{N} w_{ij} \xi_j^\lambda, \quad \text{for } i = 1,\cdots, N,\ \lambda = 1,\cdots, P \tag{3}$$

When we solved Eq. (3) for $w_{ij}$, we obtained

$$w_{ij} = \frac{1}{N} \sum_{v=1}^{P} \sum_{\mu=1}^{P} \xi_i^\mu (\mathbf{Q}^{-1})_{\mu v} \xi_j^v, \quad \text{for } i, j = 1,\cdots, N \tag{4}$$

where $\mathbf{Q}$ was a $P \times P$ overlap matrix defined as

$$\mathbf{Q}_{\mu v} = \frac{1}{N} \sum_{i=1}^{N} \xi_i^\mu \xi_i^v, \quad \text{for } \mu, v = 1,\cdots,P \tag{5}$$

After we inputted a test image to the trained HM to initialize $u_i$ values, the HM eventually reached equilibrium. An associated image in the equilibrium is not necessarily the same as any of the supervisory images but is instead one of the linear combinations of the supervisory images, so that the variety corresponding to the test image cannot be determined simply. In such a case, the variety of the test image was determined to be a variety of the $\Lambda$th supervisory image, assuming that $\zeta$ satisfied the following equation:

$$\frac{N\sum_{i=1}^{N}\xi_i^\Lambda\eta_i - \sum_{i=1}^{N}\xi_i^\Lambda\sum_{i=1}^{N}\eta_i}{\sqrt{N\sum_{i=1}^{N}(\xi_i^\Lambda)^2 - \left(\sum_{i=1}^{N}\xi_i^\Lambda\right)^2}} = \max_\lambda \frac{N\sum_{i=1}^{N}\xi_i^\lambda\eta_i - \sum_{i=1}^{N}\xi_i^\lambda\sum_{i=1}^{N}\eta_i}{\sqrt{N\sum_{i=1}^{N}(\xi_i^\lambda)^2 - \left(\sum_{i=1}^{N}\xi_i^\lambda\right)^2}}, \quad \text{for } \lambda = 1,\cdots, P \tag{6}$$

where $\eta_i$ was the $i$th pixel of the associated image.

The SP consisted of an input and output layer on which the linear units were arranged in this study. The numbers of input and output units were the same as the number of pixels of the input image and training varieties, respectively. The dynamics of the SP were expressed as

$$u_i^1 = \xi_i^\lambda, \quad \text{for } i = 1, \cdots, N, \ \lambda = 1, \cdots, P \tag{7}$$

$$u_i^2 = \sum_{j=1}^{N} w_{ij} u_j^1, \quad \text{for } i = 1, \cdots, P \tag{8}$$

where $N$ was the number of pixels, $P$ was the number of training varieties, $u_i^l$ was an output of the $i$th unit on the $l$th layer (the input layer was the first layer and the output layer was the second layer), $w_{ij}$ was the connection strength from the $j$th input unit to the $i$th output unit, and $\xi_i^\lambda$ was the $i$th pixel value of the $\lambda$th supervisory image. The SP was trained to map the supervisory images onto the target output variables. Assuming that $\xi_i^\lambda$ was the $i$th target output variable of the $\lambda$th supervisory image, we set the target output variables to be

$$\zeta_i^\lambda = \begin{cases} +1, & \text{if } i = \lambda \\ -1, & \text{if } i \neq \lambda \end{cases}, \quad \text{for } i, \lambda = 1, \cdots, P \tag{9}$$

and the relationship between the supervisory image and the target output was expressed as

$$\zeta_i^\lambda = \sum_{j=1}^{N} w_{ij} \xi_j^\lambda, \quad \text{for } i, \lambda = 1, \cdots, P \tag{10}$$

When we solved Eq. (10) for $w_{ij}$, we obtained

$$w_{ij} = \frac{1}{N} \sum_{\nu=1}^{P} \sum_{\mu=1}^{P} \zeta_i^\mu (\mathbf{Q}^{-1})_{\mu\nu} \xi_j^\nu, \quad \text{for } i = 1, \cdots, P, \ \ j = 1, \cdots, N \tag{11}$$

where $\mathbf{Q}$ was an overlap matrix defined as Eq. (5). When we inputted a test image to the trained SP, the SP outputted $P$ output variables. The output variables were not always the same as the target output variables of one of the trained varieties. Therefore, the variety of the test image was determined to be a variety of the $\Lambda$th supervisory image, assuming that $\Lambda$ satisfied the following equation:

$$\eta_\Lambda = \max_\lambda \ \eta_\lambda, \quad \text{for } \lambda = 1, \cdots, P \tag{12}$$

where $\eta_\lambda$ was the $\lambda$th output variable of the test image.

We trained the neural networks with either the MLSs or the LSDs, examining the number of training varieties that the neural networks could learn. We started to train the neural networks with two varieties and then increased the number of training varieties to 5, 10, 15, 20, 25, 30, 35 and 38. We chose varieties whose leaflet shapes were the most dissimilar to each other as the supervisory data set. The dissimilarities in leaflet shape were based on differences between the average first principal components of the standardized elliptic Fourier coefficients within a variety because they explained 88.5% of the leaflet shape variations (Furuta et al., 1995). Fig. 2 shows the LSD images of the training varieties.

We trained the neural networks on all combinations of the number of training varieties (from two to 38), the network architecture (either the HM or SP), the supervisory data (either the MLS or LSD), and the image size (either $16 \times 16$, $32 \times 32$ or $64 \times 64$ pixels). We inputted the ILS images to the trained neural networks and examined them by discriminant error. We called this discriminant error fitting error.

There was a possibility that we had underestimated the discriminant error because the supervisory images were based on the individual leaflet data used for the test data. Therefore, we had to examine the predictability of the neural networks using cross validation (CV). We separated 364 leaflet contours into one contour for test data and 363 contours for supervisory data. We obtained one ILS image from the one contour and 38 MLS and LSD images from the 363 contours. After we trained the neural networks with the MLSs and LSDs, we examined whether the neural networks could correctly discriminate varieties of ILS. We repeated this process so that each individual leaflet contour was used as the test image once. In this study, CV error indicates the discriminant error based on CV.

## 3. Results and discussion

The neural networks could learn the 38 varieties under all the training conditions except the cases of the training with more than 30 varieties using MLS images with $16 \times 16$ pixels. Only two gray levels and the low resolution of the supervisory images caused learning failure because the inverse of the matrix $\mathbf{Q}$ in Eqs. (4) and (11) did not exist.

The fitting error and CV error from the model in this study were summarized in Tables 1 and 2, respectively. Figs. 3 and 4 show the two types of discriminant errors. Note that the errors from the neural networks that failed to learn were not plotted.

The SPs trained with LSD images of $32 \times 32$ or $64 \times 64$ pixels were superior to those trained under other conditions with respect to the fitting error (Fig. 3). The LSD images of $32 \times 32$ or $64 \times 64$ pixels were more expressive at describing the inter-varietal variation than the MLS or the $16 \times 16$-pixel images. The fitting errors were lower under the SP than the HM, under the LSD than the MLS, and under the $32 \times 32$- or $64 \times 64$-pixel images than the $16 \times 16$-pixel images. The fitting error strongly depended on the training conditions.

On the other hand, the CV error did not depend on either the network architecture or the supervisory data, but only the number of training varieties and the image size (Fig. 4).

The fitting error without exception did not exceed the CV error. This indicates an overfitting of the training process. The SPs trained with LSD images were overfit in particular because the CV error did not depend on the neural network architecture and the supervisory data. It is supposed that the small sample size within a variety

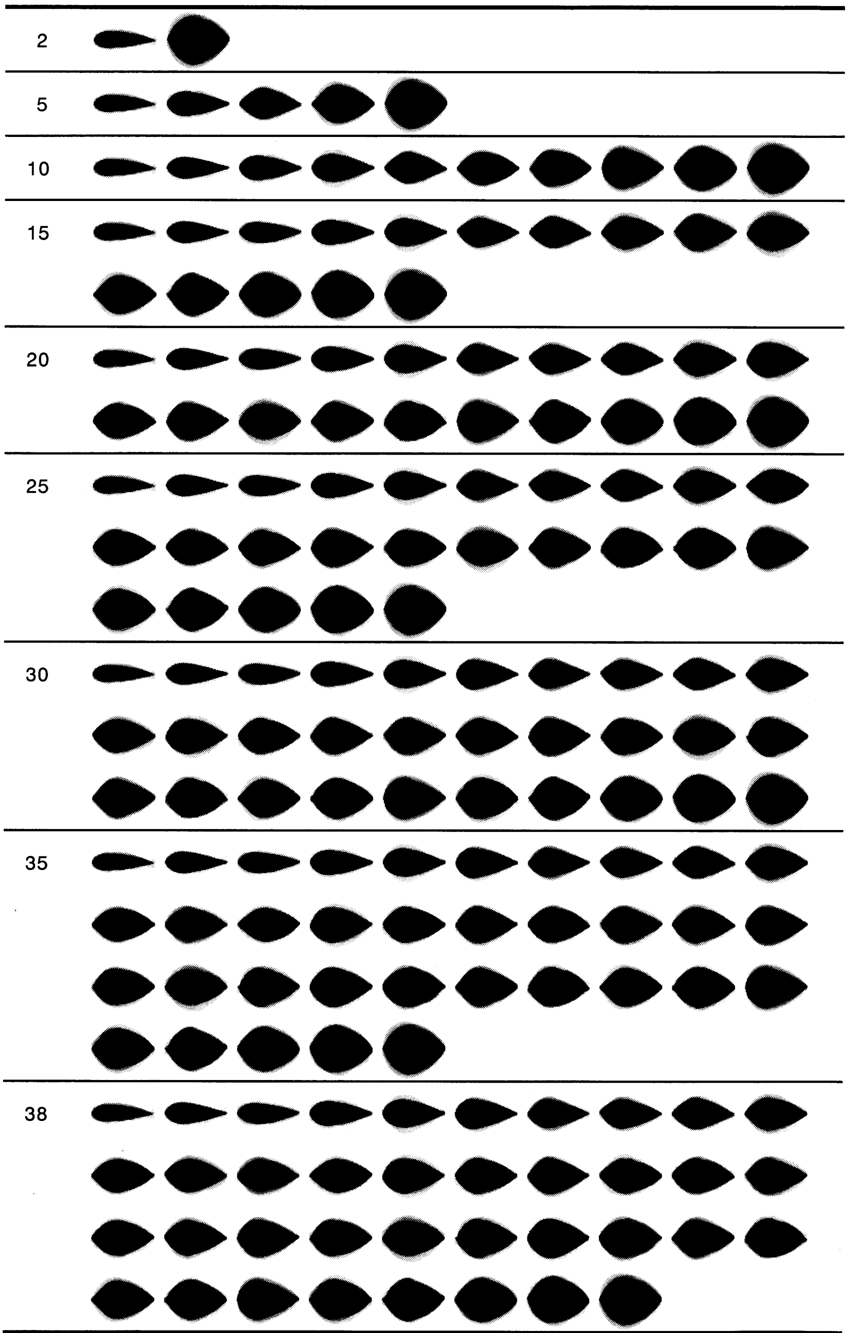


Fig. 2. Leaflet shape distribution of the training varieties arranged in order of the average first principal component of the standardized elliptic Fourier coefficients within a variety. Numerical values on the left side show the number of training varieties. Notice that, the larger the number of training varieties was, the smaller the inter-varietal leaflet shape discrepancy between the neighboring varieties became.

Table 1
Fitting errors under the combination of the training conditions[a]

| Training conditions | | | Number of training varieties | | | | | | | | |
|---|---|---|---|---|---|---|---|---|---|---|---|
| Image size | Network architecture | Supervisory data | 2 | 5 | 10 | 15 | 20 | 25 | 30 | 35 | 38 |
| 16×16 | HM | MLS | 0.00 | 0.0392 | 0.255 | 0.460 | 0.545 | 0.572 | 0.625 | – | – |
| | | LSD | 0.00 | 0.0392 | 0.225 | 0.367 | 0.390 | 0.424 | 0.469 | 0.493 | 0.516 |
| | SP | MLS | 0.00 | 0.0392 | 0.255 | 0.447 | 0.590 | 0.609 | 0.712 | – | – |
| | | LSD | 0.00 | 0.0392 | 0.167 | 0.267 | 0.267 | 0.346 | 0.399 | 0.439 | 0.475 |
| 32×32 | HM | MLS | 0.00 | 0.0588 | 0.196 | 0.400 | 0.436 | 0.490 | 0.538 | 0.552 | 0.574 |
| | | LSD | 0.00 | 0.0588 | 0.196 | 0.327 | 0.338 | 0.362 | 0.420 | 0.451 | 0.456 |
| | SP | MLS | 0.00 | 0.0588 | 0.206 | 0.387 | 0.426 | 0.506 | 0.583 | 0.602 | 0.621 |
| | | LSD | 0.00 | 0.0588 | 0.127 | 0.193 | 0.169 | 0.173 | 0.184 | 0.184 | 0.187 |
| 64×64 | HM | MLS | 0.00 | 0.0588 | 0.196 | 0.373 | 0.421 | 0.477 | 0.542 | 0.567 | 0.571 |
| | | LSD | 0.00 | 0.0588 | 0.196 | 0.313 | 0.323 | 0.337 | 0.389 | 0.421 | 0.426 |
| | SP | MLS | 0.00 | 0.0588 | 0.176 | 0.333 | 0.395 | 0.453 | 0.503 | 0.555 | 0.563 |
| | | LSD | 0.00 | 0.0588 | 0.118 | 0.200 | 0.154 | 0.165 | 0.156 | 0.139 | 0.137 |

[a] HM, Hopfield model; SP, simple perceptron; MLS, mean leaflet shape; LSD, leaflet shape distribution. A dash shows that the discriminant error was not obtained because of learning failure.

Table 2
Cross validation errors under the combination of the training conditions[a]

| Training conditions | | | Number of training varieties | | | | | | | | |
|---|---|---|---|---|---|---|---|---|---|---|---|
| Image size | Network architecture | Supervisory data | 2 | 5 | 10 | 15 | 20 | 25 | 30 | 35 | 38 |
| 16 × 16 | HM | MLS | 0.00 | 0.0784 | 0.294 | 0.520 | 0.605 | 0.634 | 0.701 | – | – |
| | | LSD | 0.00 | 0.0784 | 0.265 | 0.527 | 0.585 | 0.621 | 0.698 | 0.697 | 0.720 |
| | SP | MLS | 0.00 | 0.0784 | 0.314 | 0.520 | 0.636 | 0.679 | 0.733 | – | – |
| | | LSD | 0.00 | 0.0784 | 0.265 | 0.540 | 0.600 | 0.695 | 0.753 | 0.772 | 0.794 |
| 32 × 32 | HM | MLS | 0.00 | 0.0588 | 0.235 | 0.513 | 0.533 | 0.576 | 0.653 | 0.665 | 0.681 |
| | | LSD | 0.00 | 0.0588 | 0.245 | 0.453 | 0.492 | 0.556 | 0.622 | 0.635 | 0.657 |
| | SP | MLS | 0.00 | 0.0588 | 0.235 | 0.473 | 0.533 | 0.576 | 0.656 | 0.659 | 0.695 |
| | | LSD | 0.00 | 0.0588 | 0.235 | 0.420 | 0.487 | 0.547 | 0.618 | 0.662 | 0.703 |
| 64 × 64 | HM | MLS | 0.00 | 0.0588 | 0.235 | 0.467 | 0.523 | 0.568 | 0.663 | 0.659 | 0.679 |
| | | LSD | 0.00 | 0.0588 | 0.245 | 0.440 | 0.492 | 0.547 | 0.618 | 0.635 | 0.665 |
| | SP | MLS | 0.00 | 0.0588 | 0.225 | 0.427 | 0.482 | 0.551 | 0.615 | 0.650 | 0.673 |
| | | LSD | 0.00 | 0.0588 | 0.225 | 0.393 | 0.436 | 0.551 | 0.611 | 0.638 | 0.679 |

[a] HM, Hopfield model; SP, simple perceptron; MLS, mean leaflet shape; LSD, leaflet shape distribution. A dash shows that the discriminant error was not obtained because of learning failure.

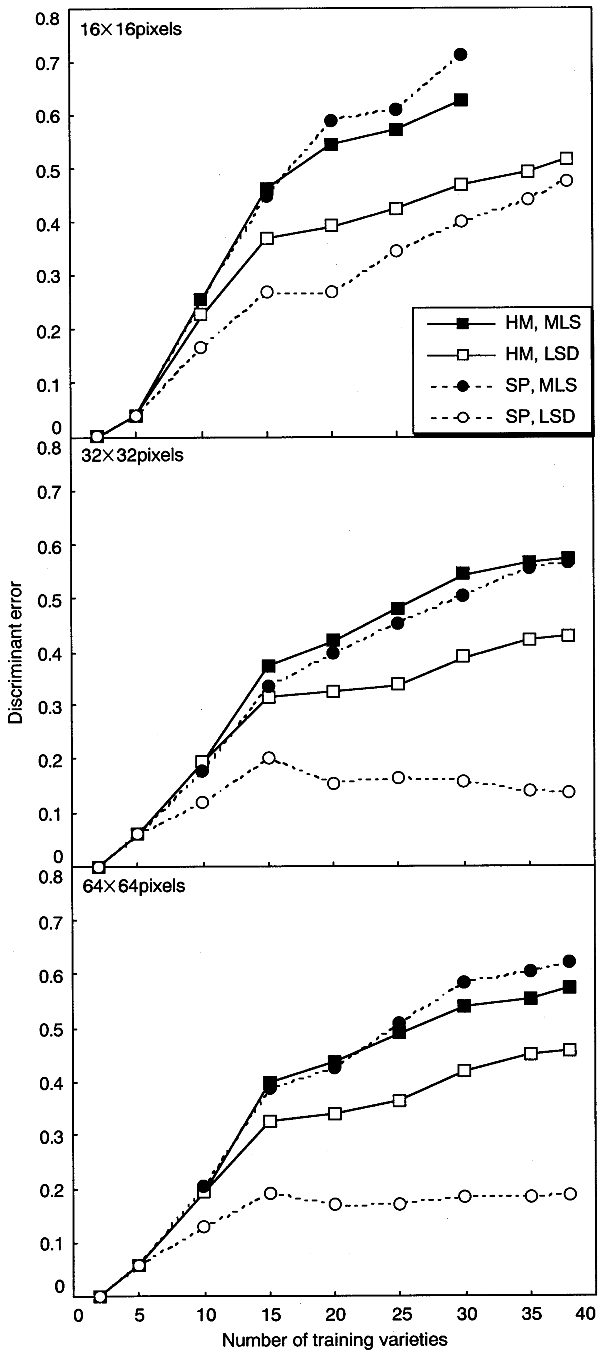


Fig. 3. Fitting error from the neural networks examined in this study. HM, Hopfield model; SP, simple perceptron; MLS, mean leaflet shape; LSD, leaflet shape distribution.

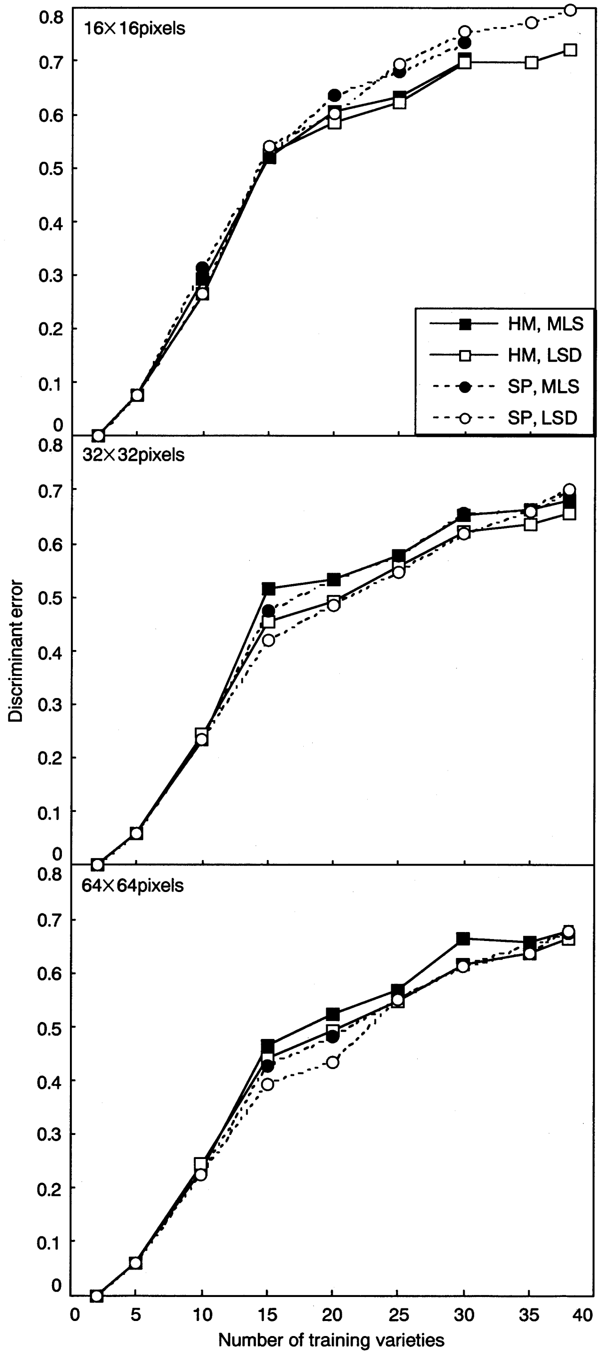


Fig. 4. Cross validation error from the neural networks examined in this study. HM, Hopfield model; SP, simple perceptron; MLS, mean leaflet shape; LSD, leaflet shape distribution.

caused the high CV errors and the overfitting. The supervisory image, which was the mean of the ILS within a variety, fluctuated largely depending on the individual leaf removed as the test data. If the sample size is large enough for the removed individual leaflet to have a weak influence on the supervisory image, the CV error is expected to be as low as the fitting error.

As the number of training varieties increased, the discriminant error was raised in most cases. It is because the intra-varietal variation can often exceed relatively small inter-varietal variation (Fig. 2), in the case of many training varieties, and some ILSs can be more similar to the supervisory data of a different variety, that the developed model could not correctly discriminate ILSs.

Considering that the inter-varietal variation was extremely small even within ten varieties (Fig. 2), the CV errors of up to ten varieties were sufficiently low under the best training conditions (the SP trained with LSD images of $64 \times 64$ pixels). The CV error of ten varieties was 0.225 under the best training conditions. This model worked quite well for quantitative varietal discrimination by soybean leaflet shape in spite of image input without any shape features. Moreover, we considered that the standardization of input data by standardized elliptic Fourier descriptors (Furuta et al., 1995) raised the discriminant efficiency because this model could purely evaluate leaf shapes that were size, rotation, and translation invariance.

The image input model had the advantage of not requiring any definition and extraction of shape features. This indicates that the model suggested in this study can be a generalized leaf shape model for various cases. This model should be especially useful when we have to consider many genetic resources. In the next study, we need to verify the applicability of this model to the evaluation of leaf shape in other cases.

We used the simplest neural network structure as the first step of the neural network examination. However, because nonlinear data processing is one of the greatest assets of neural networks, neural networks with more complex structure (e.g. MLP) may be able to improve their discriminant ability. In future work, we need to study such neural network structures to make the best use of the neural network's assets.

## References

Carneiro, L.C., Lima, M.B., 1987. Ampelographic characterization of grapevine varieties using leaf shape. Ciència Tèc. Vitiv. 6 (2), 67–78.

Dickinson, T.A., Parker, W.H., Strauss, R.E., 1987. Another approach to leaf shape comparisons. TAXON 36, 1–20.

Fujita, H., Katafuchi, T., Uehara, T., Nishimura, T., 1992. Application of artificial neural network to computer-aided diagnosis of coronary artery disease in myocardial SPECT bull's-eye images. J. Nucl. Med. 33, 272–276.

Furuta, N., Ninomiya, S., Takahashi, N., Ohmori, H., Ukai, Y., 1995. Quantitative evaluation of soybean (*Glycine max* L. Merr.) leaflet shape by principal component scores based on elliptic Fourier descriptor. Breed. Sci. 45, 315–320.

Gerber, D.T., Les, D.H., 1994. Comparison of leaf morphology among submersed species of *Myriophyllum* (Haloragaceae) from different habitats and geographical distributions. Am. J. Bot. 81, 973–979.

Guyer, D.E., Miles, G.E., Gaultney, L.D., Schreiber, M.M., 1993. Application of machine vision to shape analysis in leaf and plant identification. Trans. ASAE 36, 163–171.

Hadipoentyanti, E., Niwa, M., Furuta, N., Ninomiya, S., 1996. Discrimination between Indonesian clove (*Syzygium aromaticum* (L.) Merr. & Perr.) populations by elliptic Fourier descriptors of leaf shape. SABRAO J. 28 (2), 25–34.

Hopfield, J.J., 1982. Neural networks and physical systems with emergent collective computational abilities. Proc. Natl. Acad. Sci. USA 79, 2554–2558.

Ingrouille, M.J., Laird, S.M., 1986. A quantitative approach to oak variability in some north London woodlands. Lond. Nat. 65, 35–46.

Jensen, R.J., 1990. Detecting shape variation in oak leaf morphology: a comparison of rotational-fit methods. Am. J. Bot. 77, 1279–1293.

Makino, T., 1961. Makino's new illustrated book of Japan flora, Hokuryu-kan, Tokyo (in Japanese).

McLellan, T., 1990. Development of differences in leaf shape in *Begonia dregei* (Begoniaceae). Am. J. Bot. 77, 323–337.

Oide, M., Ninomiya, S., 1998. Evaluation of soybean plant shape by multilayer perceptron with direct image input. Breed. Sci. 48, 257–262.

Ray, T.S., 1992. Landmark eigenshape analysis: homologous contours: leaf shape in *Syngonium* (Araceae). Am. J. Bot. 79, 69–76.

Rosenblatt, F., 1962. Principles of Neurodynamics. Spartan Books, New York.

Rumelhart, D.E., McClelland, J.L., The PDP Research Group 1986. Parallel distributed processing, Volumes 1 & 2. MIT Press, Cambridge, MA.

Sawada, S., 1992. Time of determination and variations within and between plants in leaf shape of soybean. Jpn. J. Crop Sci. 61, 96–100.

Wu, H., 1994. Allometrical growth of the quantitative characters of plants 1. Measurement of leaf size and shape. Bot. Bull. Acad. Sin. 35, 115–124.

Yonekawa, S., Sakai, N., Kitani, O., 1996. Identification of idealized leaf types using simple dimensionless shape factors by image analysis. Trans. ASAE 39, 1525–1533.